

A Solution of the Maxwell-Dirac Equations in 3+1 Dimensions

A. Garrett Lisi

Department of Physics, University of California San Diego, La Jolla, CA 92093-0319

(October 31, 1994)

Abstract

We investigate a class of localized, stationary, particular numerical solutions to the Maxwell-Dirac system of classical nonlinear field equations. The solutions are discrete energy eigenstates bound predominantly by the self-produced electric field.

1994 PACS numbers: 03.65.Ge, 13.10.+q, 11.15.-q, 02.60.Cb

I. INTRODUCTION

There are many examples of classical solitary wave solutions to nonlinear field theory equations. Some of these are useful in quantum field theory as a stationary point in the action functional about which one quantizes the field [1]. Although these solutions are often relegated to model equations in fewer than three space dimensions [2], we consider the Maxwell-Dirac system of equations in 3+1 dimensional space-time, a nonlinear system of PDE's involving twelve real functions of four variables. The general solution of this system is certainly well beyond our grasp; however, we will obtain a class of particular solutions by making simplifying assumptions and utilizing numerical methods.

Before we embark on a search for a localized solution it would be wise to consider on what grounds such a solution is plausible. It is well known that when one considers the Dirac equation with an external “repulsive” potential the possibility arises to obtain bound state solutions [3]. This potential produces bound states with discrete energies that rise from the continuum of free negative energy states in the same way that an “attractive” potential produces lower energy states from those of positive energy. For a great enough “repulsive” potential we may even obtain bound states of positive energy. This interesting phenomenon goes under the name of “Klein’s paradox” and provides our motivation. In our case the “repulsive” potential is provided by the charge feeling its own electric field.

II. FIELD EQUATIONS

The Maxwell-Dirac equations are obtained from the Lagrangian density

$$L = i\bar{\Psi}\gamma^\mu\partial_\mu\Psi - \bar{\Psi}\Psi - q\bar{\Psi}\gamma^\mu\Psi A_\mu - \frac{1}{4}F^{\mu\nu}F_{\mu\nu}, \quad (2.1)$$

in which the c-number fields are the Dirac spinor Ψ , which can be considered a four component single-column matrix, and we have $A^\mu = (\Phi, \vec{A})$, $\bar{\Psi} \equiv \Psi^\dagger\gamma^0$, $F^{\mu\nu} \equiv \partial^\mu A^\nu - \partial^\nu A^\mu$, $\partial_\mu \equiv \frac{\partial}{\partial x^\mu}$, $x^\mu = (t, \vec{x})$, and γ^μ are the 4×4 matrices

$$\gamma^0 \equiv \begin{pmatrix} I & 0 \\ 0 & -I \end{pmatrix}, \vec{\gamma} \equiv \begin{pmatrix} 0 & \vec{\sigma} \\ -\vec{\sigma} & 0 \end{pmatrix},$$

in which I is the 2×2 identity matrix and $\vec{\sigma}$ represents the Pauli matrices

$$\sigma_x \equiv \begin{pmatrix} 0 & 1 \\ 1 & 0 \end{pmatrix}, \sigma_y \equiv \begin{pmatrix} 0 & -i \\ i & 0 \end{pmatrix}, \sigma_z \equiv \begin{pmatrix} 1 & 0 \\ 0 & -1 \end{pmatrix}.$$

The Euler-Lagrange equations applied to Eq. (2.1) give the Maxwell-Dirac equations

$$\gamma^\mu (i\partial_\mu - qA_\mu)\Psi - \Psi = 0, \quad (2.2)$$

$$\partial_\nu F^{\mu\nu} = q\bar{\Psi}\gamma^\mu\Psi. \quad (2.3)$$

Throughout we use natural units, in which we have rescaled length, mass, and time so that $\hbar = m = c = 1$.

We now begin making assumptions about the solution we wish to look for. We require that A^μ satisfy the Lorentz condition $\partial_\mu A^\mu = 0$ and that Ψ is an energy eigenstate, $\Psi = \psi(\vec{x})e^{-iEt}$. Equation (2.3) now reduces to Poisson's equation

$$\nabla^2 A^\mu = -j^\mu, \quad (2.4)$$

where j^μ is the 4-current

$$j^\mu = q\bar{\psi}\gamma^\mu\psi, \quad (2.5)$$

and Eq. (2.2) can be written as a Hamiltonian eigenvalue equation

$$E\psi = H\psi = [\gamma^0\vec{\gamma} \cdot (-i\vec{\nabla} - q\vec{A}) + \gamma^0 + q\Phi]\psi. \quad (2.6)$$

We would now like to assume spherical symmetry for our wave function; however, we find that the resulting vector potential \vec{A} has an angular dependence that destroys the symmetry. This gives us two options: we may throw out the magnetic term in the hope that its contribution will be small and solve the resulting one dimensional, spherically symmetric problem, or we may attack the non-spherical problem. We proceed with the former and

save the latter for Sec. V. By removing \vec{A} we reduce the Maxwell-Dirac system (2.1) to a massless scalar-Dirac system

$$L = i\bar{\Psi}\gamma^\mu\partial_\mu\Psi - \bar{\Psi}\Psi - q\bar{\Psi}\gamma^0\Psi\Phi + \frac{1}{2}(\partial_\mu\Phi)(\partial^\mu\Phi). \quad (2.7)$$

Note that, with γ^0 in the coupling term, our massless scalar-Dirac system (2.7) is not Lorentz invariant and is therefore only of use in approximating the Maxwell-Dirac system.

The necessity for a spherical charge distribution restricts our wavefunction to four possible configurations corresponding to total angular momentum up or down, $m_z = \pm\frac{1}{2}$, and the quantum number $\kappa = \pm 1$,

$$\begin{aligned} \kappa = -1 \\ m_z = \frac{1}{2} \quad \text{for } \psi = & \begin{pmatrix} g(r) \\ 0 \\ -if(r)\cos\theta \\ -if(r)e^{i\phi}\sin\theta \end{pmatrix}, \\ \kappa = 1 \\ m_z = \frac{1}{2} \quad \text{for } \psi = & \begin{pmatrix} g(r)\cos\theta \\ g(r)e^{i\phi}\sin\theta \\ -if(r) \\ 0 \end{pmatrix}, \\ \kappa = -1 \\ m_z = -\frac{1}{2} \quad \text{for } \psi = & \begin{pmatrix} 0 \\ g(r) \\ -if(r)e^{-i\phi}\sin\theta \\ if(r)\cos\theta \end{pmatrix}, \\ \kappa = 1 \\ m_z = -\frac{1}{2} \quad \text{for } \psi = & \begin{pmatrix} g(r)e^{-i\phi}\sin\theta \\ -g(r)\cos\theta \\ 0 \\ -if(r) \end{pmatrix}, \end{aligned} \quad (2.8)$$

in spherical coordinates (r, θ, ϕ) , where we have chosen to orient the angular momentum along the z-axis. Note that the two $\kappa = -1$ configurations have the same angular dependence as the Hydrogen ground state. Equations (2.4-2.6), neglecting \vec{A} , now reduce to the radial equations

$$E \begin{pmatrix} g \\ f \end{pmatrix} = \begin{pmatrix} q\Phi + 1 & -\frac{d}{dr} + \frac{\kappa-1}{r} \\ \frac{d}{dr} + \frac{\kappa+1}{r} & q\Phi - 1 \end{pmatrix} \begin{pmatrix} g \\ f \end{pmatrix}, \quad (2.9)$$

$$\Phi'' + \frac{2}{r}\Phi' = -q(f^2 + g^2). \quad (2.10)$$

We symmetrize the Hamiltonian in Eq. (2.9) by the similarity transformation $F \equiv rf, G \equiv rg$, and further simplify Eqs. (2.9) and (2.10) by identifying the fine structure constant $\alpha \equiv \frac{q^2}{4\pi}$ and defining the potential $V \equiv q\Phi$, giving us

$$E \begin{pmatrix} G \\ F \end{pmatrix} = \begin{pmatrix} V + 1 & -\frac{d}{dr} + \frac{\kappa}{r} \\ \frac{d}{dr} + \frac{\kappa}{r} & V - 1 \end{pmatrix} \begin{pmatrix} G \\ F \end{pmatrix}, \quad (2.11)$$

$$(rV)'' = -\frac{4\pi\alpha}{r}(F^2 + G^2). \quad (2.12)$$

We also restrict our wavefunction by imposing the normalization condition

$$1 = \int d^3x \Psi^\dagger \Psi = 4\pi \int_0^\infty dr (F^2 + G^2), \quad (2.13)$$

ensuring a total charge of q . Note that m_z does not appear in Eqs. (2.11-2.13); hence the energy levels are independent of the choice $m_z = \pm\frac{1}{2}$.

III. SOLUTION

We may readily solve our system of O.D.E.'s (2.11, 2.12) by a variety of means, including power series solution [4], Padé series approximation [5], and numerical methods. We choose the latter as it seems the most straightforward path to obtaining a solution.

We discretize Eqs. (2.11) and (2.12) using second order finite differences to obtain a standard, linear, symmetric, matrix eigenvalue problem for $(G(r), F(r))$ and E coupled nonlinearly to a symmetric, matrix inverse problem for rV . We obtain solutions by solving each linear problem independently and iterating to convergence from an initial guess. This technique is similar to Newton's method of solving the nonlinear system but allows for better behavior in solving the eigenvalue problem at the cost of slower convergence. We use inverse iteration for the eigenvalue problem together with the conjugate gradient method [6] for the matrix inverses. Although more efficient methods are available for the one dimensional

problem [7], we have chosen methods which will work equally well for the case of two independent variables discussed in Sec. V.

Figure 1 shows a solution to our system (2.11-2.13) for the choice of $\alpha = 2.7$. We may use the numerical solution to calculate expectation values, such as $\langle r \rangle$ and the strength of the neglected magnetic interaction. Table I shows the results for various selections of the parameter α , which completely determines the set of solutions. The energy E as a function of α , κ , and the number of nodes in g , represented by n , is shown in Fig. 2. We can see from Fig. 2 and directly from Eq. (2.11) that localized solutions are only possible for $-1 < E < 1$. Note that positive energy solutions exist for $\alpha > 2.4$ and that there is a spectrum of large n states of energies near negative one for any choice of α .

IV. MAGNETIC INTERACTION PERTURBATION

For the solution to our scalar-Dirac equations to be a viable approximate solution to the Maxwell-Dirac equations, we must establish that the inclusion of the magnetic interaction does not significantly alter the solution. We do this properly in Sec. V by modeling the larger system (2.4-2.6), including the angular dependence; however, we will use perturbation theory with our spherically symmetric solution to determine the approximate energy shift ΔE_M due to the magnetic interaction and find good agreement with the full Maxwell-Dirac case.

The magnetic interaction term in the Hamiltonian density is

$$H_M = -\vec{j} \cdot \vec{A}. \quad (4.1)$$

We use our solution form (2.8) in Eq. (2.5) to get the current

$$\vec{j} = 4q\kappa m_z f(r)g(r) \sin\theta \hat{\phi}. \quad (4.2)$$

From this we obtain the vector potential $\vec{A} = A(r) \sin\theta \hat{\phi}$, in which A is calculated via the Green's function integral

$$A(r) = \frac{1}{3} \int_0^\infty dr_1 r_1^2 \frac{r_{<}}{r_{>}^2} j(r_1), \quad (4.3)$$

where $r_<$ ($r_>$) represents the lesser (greater) of r and r_1 . We may now calculate the approximate magnetic energy shift to first order via

$$\begin{aligned}\Delta E_M &\simeq \int d^3x H_M \\ &= -\frac{128}{9}\pi^2\alpha \int_0^\infty dr F(r)G(r) \int_0^\infty dr_1 \frac{r_<}{r_>^2} F(r_1)G(r_1).\end{aligned}\tag{4.4}$$

The values obtained for ΔE_M are seen in Fig. 2 and Table I and found to be small compared to the binding energy.

We may also use our current (4.2) to calculate the magnetic moment via

$$\begin{aligned}\vec{\mu} &= \frac{1}{2} \int d^3x (\vec{x} \times \vec{j}) \\ &= 2q\kappa m_z \pi^2 \int_0^\infty dr r F(r)G(r) \hat{z}.\end{aligned}\tag{4.5}$$

Note in Table I that we obtain the result $|\mu_z| \simeq \frac{q}{2}$ when we choose $\kappa = 1$.

V. FULL MAXWELL-DIRAC SOLUTION

From our calculations in the previous section we expect that the inclusion of the magnetic interaction will result in the emergence of a small non-trivial angular dependence on the θ coordinate. We also expect the solution to maintain its axial symmetry and proceed in cylindrical coordinates (ρ, z, ϕ) , assuming a wavefunction of the form

$$\psi = \begin{pmatrix} \psi_1(\rho, z)e^{i(m_z - \frac{1}{2})\phi} \\ \psi_2(\rho, z)e^{i(m_z + \frac{1}{2})\phi} \\ -i\psi_3(\rho, z)e^{i(m_z - \frac{1}{2})\phi} \\ -i\psi_4(\rho, z)e^{i(m_z + \frac{1}{2})\phi} \end{pmatrix}\tag{5.1}$$

and potentials of the form $\Phi = \frac{1}{q}V(\rho, z)$, $\vec{A} = \frac{1}{q}A(\rho, z)\hat{\phi}$. Equations (2.4-2.5) now reduce to

$$(\partial_\rho^2 + \frac{1}{4\rho^2} + \partial_z^2)(\sqrt{\rho}V) = -4\pi\alpha\sqrt{\rho}(\psi_1^2 + \psi_2^2 + \psi_3^2 + \psi_4^2),\tag{5.2}$$

$$(\partial_\rho^2 - \frac{3}{4\rho^2} + \partial_z^2)(\sqrt{\rho}A) = 8\pi\alpha\sqrt{\rho}(\psi_1\psi_4 - \psi_2\psi_3),\tag{5.3}$$

and the Hamiltonian (2.6) becomes

$$E \begin{pmatrix} V+1 & 0 & -\partial_z & -\partial_\rho - \frac{(m_z + \frac{1}{2})}{\rho} + A \\ 0 & V+1 & -\partial_\rho + \frac{(m_z - \frac{1}{2})}{\rho} - A & \partial_z \\ \partial_z & \partial_\rho + \frac{(m_z + \frac{1}{2})}{\rho} - A & V-1 & 0 \\ \partial_\rho - \frac{(m_z - \frac{1}{2})}{\rho} + A & -\partial_z & 0 & V-1 \end{pmatrix}. \quad (5.4)$$

We symmetrize (5.4) by the substitution $\Psi_\alpha \equiv \sqrt{\rho}\psi_\alpha$, giving us

$$E \begin{pmatrix} \Psi_1 \\ \Psi_2 \\ \Psi_3 \\ \Psi_4 \end{pmatrix} = \begin{pmatrix} V+1 & 0 & -\partial_z & -\partial_\rho - \frac{m_z}{\rho} + A \\ 0 & V+1 & -\partial_\rho + \frac{m_z}{\rho} - A & \partial_z \\ \partial_z & \partial_\rho + \frac{m_z}{\rho} - A & V-1 & 0 \\ \partial_\rho - \frac{m_z}{\rho} + A & -\partial_z & 0 & V-1 \end{pmatrix} \begin{pmatrix} \Psi_1 \\ \Psi_2 \\ \Psi_3 \\ \Psi_4 \end{pmatrix}. \quad (5.5)$$

Note that our wavefunctions in both cases (2.8) and (5.1) are eigenfunctions of the z component of the angular momentum J_z with eigenvalue $m_z = \pm\frac{1}{2}$, where

$$J_z \equiv L_z + \frac{1}{2}\Sigma_z, \quad (5.6)$$

in which $\vec{L} \equiv -i(\vec{x} \times \vec{\nabla})$ and

$$\vec{\Sigma} \equiv \begin{pmatrix} \vec{\sigma} & 0 \\ 0 & \vec{\sigma} \end{pmatrix}. \quad (5.7)$$

The full system (5.2-5.5) is once again spin degenerate since the change to $m_z = -m'_z$ produces the same system with the change ($A = -A'$, $\Psi_1 = -\Psi'_2$, $\Psi_2 = \Psi'_1$, $\Psi_3 = \Psi'_4$, $\Psi_4 = -\Psi'_3$). Although our scalar-Dirac wavefunctions (2.8) are eigenfunctions of $K \equiv \gamma^0(\vec{\sigma} \cdot \vec{L} + 1)$ with eigenvalue κ , our solutions of the non-spherically symmetric case will vary slightly from these eigenfunctions.

Figure 3 shows a numerical solution to the full system for the same parameter choice as in Fig. 1. Note that the angular dependence is virtually indistinguishable from the approximate solution and that the energy agrees reasonably well with the first order perturbation approximation.

VI. CONCLUSION

We have found a class of solutions to the full Maxwell-Dirac equations and good approximate solutions via a scalar-Dirac equation. In practice, the approximate solution is easier

to work with and provides better accuracy for most calculations.

The issue of stability has not been directly addressed. The success of our iterative solution method suggests that each solution is stable in regard to slow collapse or expansion; however, we suspect that each solution will be unstable via radiative transitions to states of large negative energy, as is any bound state solution to the Dirac equation.

The interpretation of our solution is not immediately clear. Several authors have used similar solutions to construct hadrons from interacting quarks [8,9]; however, these solutions were to systems of nonlinear scalar fields interacting with the Dirac field and the solutions were essentially a result of the nonlinear scalar self-interaction rather than the coupling term. As it exists now, we see that our class of solutions to the Maxwell-Dirac system may not be immediately interpreted as representing the leptons. This is clear from the large value of $\langle r \rangle$ and negative value for E for $\alpha = \frac{1}{137}$ as well as from the experimental fact that weak interactions play the starring role in lepton transitions. It is not inconceivable that our solution could represent the leptons if we rework our analysis to accommodate the weak interaction. Such an undertaking would present an interesting avenue for future work.

ACKNOWLEDGMENTS

I would like to express my appreciation to Roger Dashen and Henry Abarbanel for their encouragement and guidance and to the Hopgood Foundation and the San Diego chapter of the ARCS Foundation for their support.

REFERENCES

- [1] R. Rajaraman, *Solitons and Instantons* (North-Holland, Amsterdam, 1982).
- [2] A. Das, J. Math. Phys. **34**, 3986 (1993).
- [3] J. J. Sakurai, *Advanced Quantum Mechanics* (Addison-Wesley, N.Y., 1967).
- [4] M. E. Rose, *Relativistic Electron Theory* (John Wiley and Sons, N.Y., 1961).
- [5] W. L. Ditto and T. J. Pickett, J. Math. Phys. **29**, 1761 (1988).
- [6] W. Press, *Numerical Recipes in C* (Cambridge University Press, N.Y., 1992).
- [7] S. Salomonson and P. Öster, Phys. Rev. A **40**, 5548 (1989).
- [8] W. L. Bardeen, M. S. Drell, M. Weinstein, and T. M. Yan, Phys. Rev. D **11**, 1094 (1975).
- [9] T. D. Lee and G. C. Wick, Phys. Rev. D **9**, 2291 (1974).

FIGURES

FIG. 1. A normalized, localized solution to our scalar-Dirac system for the choice of $\alpha = 2.7$, $\kappa = 1$, and $n = 0$, showing $f(r)$, $g(r)$, and $V(r)$ scaled down by a factor of 6 to be fully visible. Note the asymptotic behavior of $V(r) \simeq \frac{\alpha}{r}$ for large r . The expectation value $\langle r \rangle$ is also shown. All values are in natural units. The one dimensional mesh was discretized into 200 points for this calculation.

FIG. 2. Energy levels as a function of α for our scalar-Dirac approximation. The dashed curves represent deviations due to the magnetic interaction calculated via the first order perturbation. All values shown are in natural units.

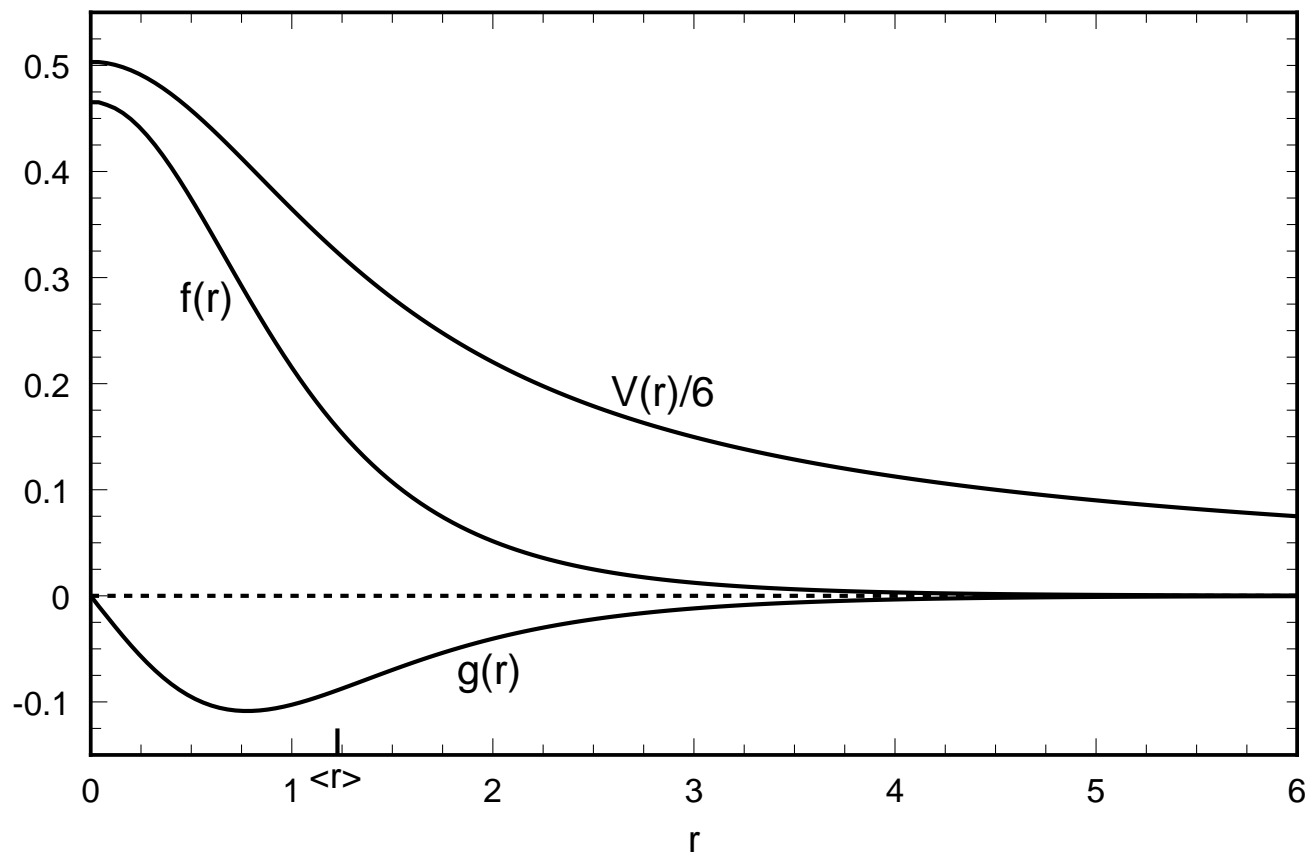
FIG. 3. A normalized, localized solution to the Maxwell-Dirac system for the choice of $\alpha = 2.7$, showing the four components of the wavefunction $\psi_i(\rho, z)$, the potential $V(\rho, z)$, and the $\hat{\phi}$ component of the vector potential $A(\rho, z)$. The contours go from min(light) to max(dark) and all values are in natural units. The two dimensional mesh was discretized into $60 \times (2 \times 60 + 1)$ points for this calculation. The energy was calculated as $E_2 = 0.22$, to be compared with that obtained from the 1-D approximation, $E + \Delta E_M = 0.30$.

TABLES

TABLE I. Numerical results for our scalar-Dirac approximation on a 200 point mesh for several choices of α , n , and κ . All values shown are in natural units.

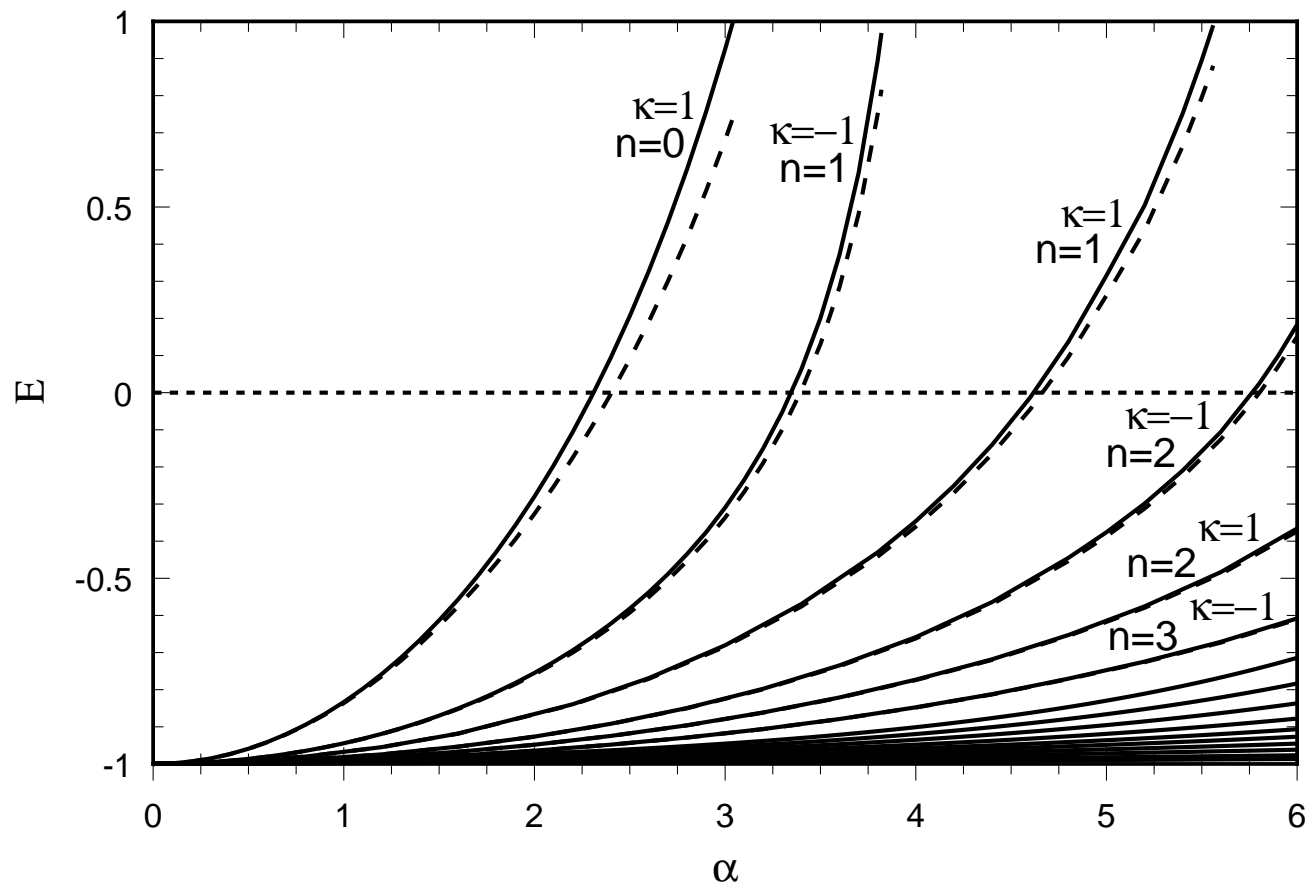
α	n	κ	E	ΔE_M	$\langle r \rangle$	$\mu_z/(qm_z)$
1/137	0	1	$-1 + 9 \times 10^{-6}$	-0.00	572	-1.2
0.1	0	1	$-1 + 2 \times 10^{-3}$	-0.00	42	-1.2
1.0	0	1	-0.83	-0.00	4.1	-1.1
2.0	0	1	-0.28	-0.05	1.9	-1.0
2.4	0	1	0.09	-0.10	1.5	-0.9
2.7 ^a	0	1	0.46	-0.16	1.2	-0.8
3.0	0	1	0.93	-0.24	1.0	-0.7
1/137	1	-1	$-1 + 3 \times 10^{-6}$	-0.00	1710	-0.4
2.0	1	-1	-0.75	-0.00	5.4	-0.3
3.4	1	-1	0.06	-0.06	2.0	-0.2
3.8	1	-1	0.89	-0.14	1.2	-0.1
3.0	1	1	-0.68	-0.00	6.2	-1.1
5.0	1	1	0.32	-0.05	2.4	-0.9
5.5	1	1	0.90	-0.10	1.8	-0.8
2.0	2	-1	-0.93	-0.00	18	-0.4
5.8	2	-1	0.02	-0.03	3.5	-0.2
6.0	2	-1	0.18	-0.03	3.1	-0.2
6.0	2	1	-0.37	-0.01	6.2	-1.0
6.0	3	1	-0.71	-0.00	13	-1.1

^aSolution shown in Fig. 1.



This figure "fig1-1.png" is available in "png" format from:

<http://arXiv.org/ps/hep-th/9410244v2>



This figure "fig1-2.png" is available in "png" format from:

<http://arXiv.org/ps/hep-th/9410244v2>